

## THE DYNAMICS OF SUPERCLUSTERS: INITIAL DETERMINATION OF THE MASS DENSITY OF THE UNIVERSE AT LARGE SCALES

H. C. FORD

University of California, Los Angeles

R. J. HARMS

University of California, San Diego

R. CIARDULLO

University of California, Los Angeles

AND

F. BARTKO

Martin Marietta Corporation, Denver

Received 1980 September 2; accepted 1980 December 16

### ABSTRACT

We have measured radial velocities of cluster members of two rich, large superclusters in order to probe the supercluster mass densities and have computed simple evolutionary models to place limits upon the mass density within each supercluster. These superclusters represent true physical associations of size  $\sim 100$  Mpc (for  $H_0 = 50 \text{ km s}^{-1} \text{ Mpc}^{-1}$ ) seen presently at an early stage of evolution. One supercluster is weakly bound, the other probably barely bound, but possibly marginally unbound. Gravity has noticeably slowed the Hubble expansion of both superclusters. We used galaxy surface-density counts and the density enhancement of Abell clusters within each supercluster to derive the ratio of mass densities of the superclusters to the mean field mass density. The results strongly exclude a closed universe. We obtain  $\Omega \lesssim 0.30$  with a preferred range  $0.06 \lesssim \Omega \lesssim 0.16$ . This preferred range for the cosmological density parameter corresponds to a mass-to-luminosity range of  $48 \lesssim M/L \lesssim 129$  in solar units.

*Subject headings:* cosmology — galaxies: clusters of — galaxies: redshifts

### I. INTRODUCTION

The existence of superclusters is now well established, both locally (de Vaucouleurs 1958, 1975) and globally (Abell 1975). Statistical studies (Bogart and Wagoner 1973; Peebles 1973, 1974; Hauser and Peebles 1973; Peebles and Hauser 1974) have shown that superclusters have transverse dimensions of order 50 Mpc ( $H_0 = 50 \text{ km s}^{-1} \text{ Mpc}^{-1}$  is used throughout this *Letter*) and typically consist of two or three rich clusters, though a few very rich superclusters appear to be comprised of 10 or more clusters (Abell 1961; Murray *et al.* 1978).

Although recent studies by Rood (1976), Gregory and Thompson (1978), and Tarenghi *et al.* (1979) have considerably improved our understanding of superclusters, fundamental questions remain unanswered. Is there sufficient matter in superclusters for gravitational forces to be important? Or, are the dynamics of a supercluster completely dominated by Hubble expansion? Rood (1976) has argued that the redshifts of nearby superclusters are caused primarily or exclusively by cosmological expansion. Abell (1961), on the other hand, has cited the radial velocities within a single supercluster as at least being consistent with the idea that gravitational interactions significantly alter the velocity field. A second question is closely related to the

first. If gravitational forces are sufficient to arrest the primordial expansion of superclusters, what is their present evolutionary state?

Measurement of cluster radial velocities provides a powerful means of answering these questions and simultaneously detecting visible and invisible matter on scales large enough to determine the cosmological density parameter  $\Omega$  (see, for example, Peebles 1976; Sargent and Turner 1977; Silk and Wilson 1979). In this *Letter* we report observations and preliminary results (based on spherically symmetric models) for the two superclusters 1451+22 = Abell 11 (Abell 1961) = MFJG 18 (Murray *et al.* 1978) and 1615+43 = MFJG 19. In subsequent papers we will present a more complete analysis of the detailed data (Harms *et al.* 1981, hereafter Paper II) and provide finding charts (Ciardullo *et al.* 1981, hereafter Paper III).

Our approach involves two steps. First, we measure radial velocities for cluster members of a supercluster from which we can derive limits upon the supercluster mass density. Second, we use surface density counts and the volume density of rich clusters to obtain the supercluster density contrast  $\langle \rho (\text{supercluster}) \rangle / \langle \rho (\text{universe}) \rangle$ . Combining these two results provides a measurement of  $\Omega$  insofar as any significant quantities of matter are clumped at least as strongly as visible matter on the size scales of superclusters.

## II. RADIAL VELOCITIES

We used the Lick Image Tube Scanner (Robinson and Wampler 1972) on the Shane 3 m telescope to measure the systemic radial velocities of rich clusters in and around superclusters 1451+22 and 1615+43. Typically we observed the three brightest galaxies projected near the center of each cluster. Such galaxies have the highest *a priori* probability of being cluster members and, by virtue of having formed or settled near the bottom of the cluster's potential well, will have the least velocity dispersion about the cluster's mean velocity.

In addition to observing the rich clusters, we searched the Palomar Observatory Sky Survey (POSS) prints for poor clusters and groups which could also serve as test particles in the supercluster's gravitational field. We selected candidates which are comparable in brightness and color to the brightest galaxies in the rich

cluster members. Approximately half of the candidates so chosen proved to be members of the superclusters. These new candidates improve the statistical significance of the results and reveal the enormous extent of the superclusters.

Figure 1 maps the member clusters in each of the two superclusters. Figure 2 shows the redshift distributions for both superclusters. The contrast in redshift space is remarkable; not a single case of ambiguous membership occurs for the 28 member clusters and 44 nonmember galaxies observed in the directions of the superclusters. The nonmember which is nearest to 1451+22 has a redshift which is 7 standard deviations from the mean. The nonmember closest to 1615+43 differs from the mean by 5 standard deviations.

The projection of the superclusters onto the sky is "elliptical" with a ratio of axes  $\sim 1.7$ . The maximum transverse dimensions are  $\gtrsim 9^\circ$  ( $\gtrsim 100$  Mpc), which is

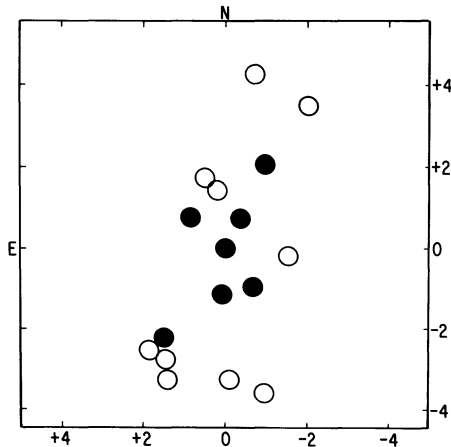


FIG. 1a

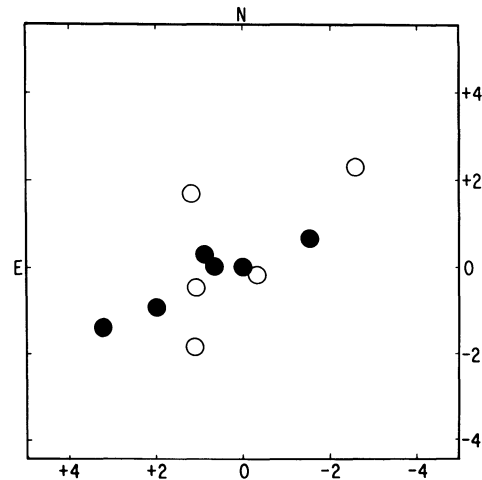


FIG. 1b

FIG. 1.—Locations of the observed supercluster members in tangential coordinates (degrees). Filled circles are Abell clusters shown scaled to Abell's (1961) defining diameters; open circles refer to member groups and poor clusters. Map origins (1950 coordinates) are: (a)  $\alpha = 14^{\text{h}} 51^{\text{m}}$ ,  $\delta = +22^\circ$  centered on Abell 1986, and (b)  $\alpha = 16^{\text{h}} 15^{\text{m}}$ ,  $\delta = +43^\circ$  centered on Abell 2172.

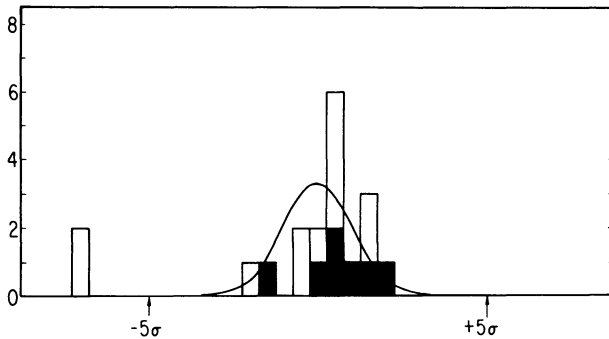


FIG. 2a

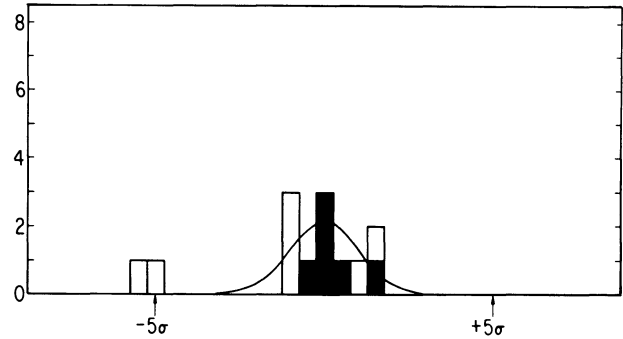


FIG. 2b

FIG. 2.—Distribution of redshifts of supercluster members and closest (in redshift) nonmember galaxies. Bins are  $\sigma/2$  wide. Filled rectangles represent Abell clusters. Open rectangles include member groups and poor clusters as well as individual nonmember galaxies. Curves are Gaussian fits to weighted data as described in the text—(a) 1451+22:  $\langle z \rangle = 0.11568$ ,  $\sigma(z) = 0.00168$ ; and (b) 1615+43:  $\langle z \rangle = 0.13502$ ,  $\sigma(z) = 0.00241$ .

more than twice the defining size used by Murray *et al.* (1978). The distributions of the Abell clusters suggest a linear morphology reminiscent of the type of structures discussed by Joeveer and Einasto (1978) and by Einasto, Joeveer, and Saar (1980). However, our data are sufficiently sparse that Monte Carlo simulations of projections of randomly placed clusters indicate about a 50% chance that these linear features are chance projections rather than intrinsic alignments.

The observed velocity dispersion of the clusters in a supercluster is slightly larger than the true velocity dispersion because of measurement uncertainty (typically  $100 \text{ km s}^{-1}$ ) and broadening by the intrinsic dispersion of galaxies within the clusters and groups. Our data give an average standard deviation  $\sigma_{\text{clusters}} = 650 \text{ km s}^{-1}$  for the rich clusters and  $\sigma_{\text{groups}} = 200 \text{ km s}^{-1}$ . The latter value is consistent with a weighted standard deviation of  $160 \text{ km s}^{-1}$  determined from the 23 groups in Turner and Gott's (1976) list, which show no evidence of contamination. We computed weighted means and weighted standard deviations using weights  $W_i = N_i \sigma_i^{-2}$ , where  $N_i$  is the number of galaxies observed in a rich cluster or group and  $\sigma_i$  is  $\sigma_{\text{cluster}}$  or  $\sigma_{\text{groups}}$ . The observed weighted standard deviations were corrected for broadening by  $\sigma_{\text{clusters}}$  and  $\sigma_{\text{groups}}$  to determine the intrinsic standard deviations ( $\sigma_0$ ) in the superclusters. Table 1 summarizes our observational results. The last column of Table 1 gives  $\sigma_0$  expressed as a velocity, omitting a cosmological correction.

### III. INTERPRETATION OF THE RADIAL VELOCITY DATA

Figure 1 shows the supercluster projections on the sky to be noncircular. Our data and those of Gregory and Thompson (1978) and Tarenghi *et al.* (1979) do suggest that superclusters, while rather irregular in shape, are not extremely aspherical (ratios of projected axes average about 1.6). In this *Letter* we calculate the implications of only those models possessing spherical symmetry and density distributions which either remain constant or decrease with increasing radius (resulting in noncrossing mass shells early in their evolution). A qualitative estimate of the effect of deviations from spherical symmetry is presented in § V.

The data indicate that matter within the superclusters has influenced cluster motions. If the observed clusters were moving solely under Hubble flow, we would observe (for a sphere) a radial velocity dispersion

$$\sigma \approx \left[ \frac{cz\theta}{\sqrt{5}} \right] \left[ 1 + \frac{(2 + \Omega)z}{4} \right], \quad (1)$$

where  $\theta$  is the apparent angular radius of the supercluster and  $z$  is its mean redshift. Using  $\theta$  (1451+22) =  $3^\circ.3$  and  $\theta$  (1615+43) =  $3^\circ.0$ , this model predicts that we should observe  $\sigma$  (1451+22) =  $946\text{--}972 \text{ km s}^{-1}$  and  $\sigma$  (1615+43) =  $1012\text{--}1044 \text{ km s}^{-1}$  in the two superclusters for  $0 \leq \Omega \leq 1$ . The probabilities that the derived true standard deviations ( $478 \text{ km s}^{-1}$  and  $720 \text{ km s}^{-1}$ ) are drawn from parent populations with  $\sigma = 960 \text{ km s}^{-1}$  and  $1030 \text{ km s}^{-1}$  are, respectively, 0.001 and 0.1. On the other hand, the matter density cannot be so high that the superclusters would virialize

in a Hubble time. Virialized superclusters would exhibit radial velocity dispersions still larger than free-Hubble-flow dispersions.

Both Rood (1976) and Wagner and Perrenod (1980) find no evidence of gravitational slowing of the Hubble flow of nearby binary and triple superclusters with density contrasts comparable to or even greater than the two superclusters discussed here. These results lead us to conclude that 1451+22 and 1615+43 have been only slightly decelerated by gravity and, if bound, have not yet reached Hubble-flow turnaround in their evolution. Consequently, we model the superclusters by noncrossing spherical mass shells (cf. Silk and Wilson 1979). We assume approximate Hubble flow initially,  $R_i = H_i V_i$  and require evolution to attain the observed parameters at the present epoch in order to determine the supercluster mass interior to a shell at  $R(t)$ .

Consider a bound spherical shell with binding energy per unit mass  $|E| = GM(R)/R - V^2/2$  evolving from initial position  $R_i$  and velocity  $V_i$  to final position  $R_f$  and velocity  $V_f$  under the influence of interior mass  $M(R)$ . Although the radius  $R$  of a shell changes with time, the mass inside the shell remains constant. Integration of the Newtonian equation of motion yields:

$$T = \left[ \frac{R_f}{2|E|} \right] \left[ \frac{(2|E| + V_f^2)}{2\sqrt{2|E|}} \left\{ \sin^{-1} \left( \frac{2|E| - V_f^2}{2|E| + V_f^2} \right) - \sin^{-1} \left[ \frac{((2|E|)(2R_i/R_f - 1) - V_f^2)}{2|E| + V_f^2} \right] \right\} - V_f + (V_i)(R_i/R_f) \right], \quad (2)$$

where  $T$  is the time for the supercluster to evolve from  $R_i$ ,  $V_i$  to  $R_f$ ,  $V_f$ . [Note that  $2|E| = (R_i V_i^2 - R_f V_f^2)/(R_f - R_i)$ .]

We solve equation (2) recursively by assuming initial values  $R_i$  and  $V_i = H_i R_i$ , and using final values  $R_f$  and  $V_f$  determined from the observations, which predicts a time  $T$ . We iterate to obtain the condition  $T = \Upsilon$ , where  $\Upsilon$  is the supercluster evolution time:

$$\Upsilon \approx \frac{1}{H_0(1+z)} - \frac{1}{H_i} \approx \frac{1}{H_0} \left( \frac{1}{1+z} - \frac{1}{1+z_i} \right), \quad (3)$$

where  $z_i$  is the Hubble-flow initial epoch and  $z$  is the observed supercluster redshift. In equation (3) we have restricted the analysis to a Friedmann cosmology with  $\Lambda = 0$  and  $\Omega$  sufficiently small that the universal deceleration can be neglected from initial epoch  $z_i$  to observed epoch  $z$ . ( $\Omega \approx 0$  agrees with the conclusions reached later in this *Letter*; the contrasting assumption of  $\Omega$  far from zero is inconsistent with the radial velocity and surface density data for the observed superclusters.)

The simultaneous solution of equations (2) and (3) provides the shell's specific binding energy  $|E|$ , thus  $M(R)$ , and ultimately the present mean matter density  $\langle \rho_{sc} \rangle$  interior to  $R$ . The result is a function of the ob-

TABLE 1  
 REDSHIFT MEANS AND STANDARD DEVIATIONS IN TWO SUPERCLUSTERS

Super-cluster	Unweighted		Weighted		$\sigma_0$	$c\sigma_0$ (km s <sup>-1</sup> )
	$z$	$\sigma(z)$	$z$	$\sigma(z)$		
1451+22.....	0.1162	$1.69 \times 10^{-3}$	0.1157	$1.68 \times 10^{-3}$	$1.59 \times 10^{-3}$	478
1615+43.....	0.1352	$2.17 \times 10^{-3}$	0.1350	$2.41 \times 10^{-3}$	$2.40 \times 10^{-3}$	720

TABLE 2  
 SUPERCLUSTER MODELS

Supercluster	Case	$H_{eff}$ (km s <sup>-1</sup> Mpc <sup>-1</sup> )	$z_i$	Age (10 <sup>9</sup> yr)	$\langle \rho_{sc} \rangle / \rho_{c0}$
1451+22.....	nominal	28.18	3	12.64	1.49
1451+22.....	young	28.18	2	11.01	1.74
1451+22.....	old	28.18	1000	17.51	1.01
1451+22.....	21% faster	34.18	3	12.64	1.08
1451+22.....	24% slower	21.50	3	12.64	1.99
1615+43.....	nominal	40.51	3	12.34	0.77
1615+43.....	young	40.51	2	10.71	0.93
1615+43.....	old	40.51	1000	17.21	0.46*
1615+43.....	26% faster	51.20	3	12.34	0.22*
1615+43.....	30% slower	28.26	3	12.34	1.58

\* Unbound solution.

served ratio  $V_r/R_f$  (an effective Hubble constant), the observed  $z$ , and the assumed  $z_i$ . In a uniformly expanding sphere, the maximum velocity is related to the radial velocity dispersion by  $V_{max} = \sqrt{5}\sigma_{sc}$ , where  $\sigma_{sc}$  is obtained from the intrinsic observed radial velocity dispersion  $\sigma_0$  by  $\sigma_{sc} = \sigma_0/(1+z)$ . The corresponding maximum radius is given by  $R_{max} = (cz\theta/\dot{H}_0)(1+z/2)/(1+z)^2$  for observed angular radius  $\theta$ .

Table 2 gives the derived densities for both superclusters for the nominal observed velocities at several initial Hubble-flow epochs  $z_i$  and for velocity extremes which symmetrically include the true parent velocities with about 80% probability. Note that the present epoch critical density  $\rho_{c0} = 4.696 \times 10^{-30}$  g cm<sup>-3</sup> (for  $H_0 = 50$ ), and that the given ratios  $\langle \rho_{sc} \rangle / \rho_{c0}$  are independent of the value for  $H_0$ .

#### IV. DENSITY ENHANCEMENTS IN SUPERCLUSTERS

We used two related techniques to measure the density enhancements in the superclusters. The first method assumes that the average density of matter on large scales is proportional to the density of rich clusters (cf. Bahcall 1979). Two normalizations were considered. Rood (1976) used the redshifts of the 27 Abell clusters in distance classes 0 to 2 to derive a density of  $6 \times 10^{-7}$  rich clusters Mpc<sup>-3</sup> (corrected to  $H_0 = 50$  km s<sup>-1</sup> Mpc<sup>-1</sup>) in a volume with radius 284 Mpc. Bahcall (1979) used the full Abell catalog of clusters with richness  $>0$  and assumed a volume corresponding to  $z(\text{maximum}) = 0.2$  and  $\Omega = 0$  to derive a luminosity function for each richness class 1 through 5. Our second method involved counting galaxies in strips across the superclusters and in nearby background regions, from which we compute the (volume)

density enhancement by using the Schechter (1976) luminosity function as normalized by Felten (1977). We included galactic absorption of  $0.16 \text{ csc } |b|$  in the E-plate bandpass, but ignored the small  $K$ -corrections and evolutionary effects in the E-plate color.

The angular radius of each supercluster was selected to encompass all of the Abell clusters and most of the groups. We corrected for space curvature (assuming  $\Omega \approx 0$ ) to the superclusters in deriving their radii. Corrections for space curvature were not included in the Schechter (1976) luminosity function, but should be small. Both rich cluster normalizations include the space curvature effects appropriate to  $\Omega = 0$ .

Each method suffers from major uncertainties: possible systematic errors in all cases and large statistical uncertainties for the rich-cluster-based determinations. We estimate the chief contributions to errors for each method to be:

1. Galaxy counts—plate density variations and fluctuations of background surface densities
2. Rood (1976) normalized Abell clusters—our small sample sizes and the assumption that the density of matter on large scales is proportional to the density of Abell clusters
3. Bahcall (1979) normalized Abell clusters—our small sample sizes, the assumed volume corresponding to  $z = 0.2$  maximum radius, and the assumption that the density of matter on large scales is proportional to the density of Abell clusters

After this, it is perhaps encouraging to see the degree of agreement of values for derived density enhancements for the superclusters presented in Table 3. The

TABLE 3  
DENSITY ENHANCEMENTS IN TWO SUPERCLUSTERS

SUPER-CLUSTER	$\theta$ (degrees)	$R(\Omega = 0)$ (Mpc)	$\langle \rho_{sc} \rangle / \rho_{field}$		GALAXY COUNTS
			RICH CLUSTERS		
			Rood	Bahcall	
1451+22..	3.3	34	71	25	17
1615+43..	3.0	35	55	18	10

galaxy surface-density measurements probably provide the best estimate for the density contrasts. In a future paper we plan to improve the spatial definition and sharpen the density contrast limits by using photoelectrically calibrated, multicolor galaxy counts.

#### V. CONCLUSIONS

For 1451+22, Table 2 shows that  $\langle \rho_{sc} \rangle / \rho_{co}$  lies between 1.01 and 1.99 allowing for reasonable uncertainties in the model parameters. When combined with the result listed in Table 3,  $17 < \langle \rho_{sc} \rangle / \rho_{field} \leq 71$ , we obtain the limit for the density of the universe  $0.01 \leq \Omega \leq 0.12$ . A similar combination of results for 1615+43 results in the limits  $0.004 \leq \Omega \leq 0.16$ . Satisfying the limits from both superclusters requires  $0.01 \leq \Omega \leq 0.12$  with a most probable range (based on the density contrasts derived from galaxy counts) given by  $0.06 \leq \Omega \leq 0.12$ .

An alternate (but nearly equivalent) method for determining  $\Omega$  from the present data has been presented by Sargent and Turner (1977). Their model assumes a uniform spherical density enhancement. They define a mean angle  $\langle \alpha \rangle$  in redshift-angular-position space to measure the departure of a density enhancement from free Hubble flow (where  $\langle \alpha \rangle \approx 32^\circ$ ). For 1451+22, we obtain  $\langle \alpha \rangle \approx (20 \pm 3)^\circ$ , and for 1615+43  $\langle \alpha \rangle \approx (27 \pm 5)^\circ$ , which is consistent with the limits on  $\Omega$  derived above.

The limits for  $\Omega$  derived above depend on the assumption of approximate spherical symmetry, or more exactly, on the assumption that the line-of-sight dimensions for the superclusters are comparable to the average projected dimensions ( $\sim 70$  Mpc diameters). Let us consider qualitatively the effect of relaxing this assumption. For a decrease in the line-of-sight supercluster thickness, the inferred slowing of the Hubble flow declines toward zero while the inferred (volume) density contrast increases, resulting in values for  $\Omega$  smaller than those calculated above. For increasing line-of-sight thickness, the inferred slowing of the Hubble flow becomes dominant, implying evolution to near turnaround corresponding to  $\langle \rho_{sc} \rangle / \rho_{co} \approx 4$ , while the inferred density contrast decreases. For line-of-sight dimensions  $\sim 100$  Mpc (edge-on disks or cigar shapes tilted about  $45^\circ$ ),  $\langle \rho_{sc} \rangle / \rho_{co} \approx 3$ , so that  $\Omega$  could be as large as  $\sim 0.3$ .

We can combine the limits for  $\Omega$  derived above with the results of Felten (1977) for the mean blue isophotal luminosity  $B(0)$  density for the universe (assuming  $H_0 = 50$ ) that  $L = 8.6 \times 10^7 L_\odot \text{ Mpc}^{-3}$  to obtain limits upon the mass-to-luminosity ratio ( $M/L$ ) for size scales larger than  $\sim 100$  Mpc. The most likely value, corresponding to  $0.06 \leq \Omega \leq 0.12$ , lies within  $48 \leq M/L \leq 97$  in solar units.

In summary, we find:

1. Physical associations of matter exist on scales up to about 100 Mpc.
2. Such superclusters have evolved only little over a Hubble time.
3. A closed universe is strongly excluded:  $\Omega \leq 0.30$ , and the most likely range is  $0.06 \leq \Omega \leq 0.12$ .
4.  $M/L$  for the universe probably lies between 48 and 97 solar units.

The authors wish to acknowledge valuable discussions with Drs. George Abell and Stephen Perrenod. This work was supported in part by NASA grant NGR-05-009-188 and NASA contract NAS 5-24463.

#### REFERENCES

- Abell, G. 1961, *A.J.*, **66**, 607.  
 ———. 1975, in *Galaxies and the Universe*, ed. A. Sandage, M. Sandage, and J. Kristian (Chicago: The University of Chicago Press), p. 601.  
 Bahcall, N. A. 1979, *A.p.J.*, **232**, 689.  
 Bogart, R. S., and Wagoner, R. V. 1973, *A.p.J.*, **181**, 609.  
 Ciardullo, R., Ford, H. C., Eason, E., Bartko, F., and Harms, R. J. 1981, *A.p.J. Suppl.*, in preparation (Paper III).  
 de Vaucouleurs, G. 1958, *A.J.*, **63**, 253.  
 ———. 1975, *A.p.J.*, **202**, 319.  
 Einasto, J., Joveer, M., and Saar, E. 1980, *M.N.R.A.S.*, submitted.  
 Felten, J. E. 1977, *A.J.*, **82**, 861.  
 Gregory, S. A., and Thompson, L. A. 1978, *A.p.J.*, **222**, 784.  
 Harms, R. J., Ford, H. C., Ciardullo, R., and Bartko, F. 1981, *A.p.J.*, in preparation (Paper II).  
 Hauser, M. G., and Peebles, P. J. E. 1973, *A.p.J.*, **185**, 757.  
 Joveer, M., and Einasto, J. 1978, in *IAU Symposium 79, The Large Scale Structure of the Universe*, ed. J. S. Longair and J. Einasto (Dordrecht: Reidel), p. 241.  
 Murray, S. S., Forman, W., Jones, C., and Giacconi, R. 1978, *A.p.J. (Letters)*, **219**, L89.  
 Peebles, P. J. E. 1973, *A.p.J.*, **185**, 413.  
 ———. 1974, *A.p.J. Suppl.*, **28**, 37.  
 ———. 1976, *A.p.J.*, **205**, 318.  
 Peebles, P. J. E., and Hauser, M. G. 1974, *A.p.J. Suppl.*, **28**, 19.  
 Robinson, L. B., and Wampler, E. J. 1972, *Pub. A.S.P.*, **84**, 161.  
 Rood, H. J. 1976, *A.p.J.*, **207**, 16.  
 Sargent, W. L. W., and Turner, E. L. 1977, *A.p.J. (Letters)*, **212**, L3.  
 Schechter, P. 1976, *A.p.J.*, **203**, 297.  
 Silk, J., and Wilson, M. L. 1979, *A.p.J.*, **228**, 641.  
 Tarenghi, M., Tift, W. G., Chincarini, G., Rood, H. J., and Thompson, L. A. 1979, *A.p.J.*, **234**, 793.  
 Turner, E. L., and Gott, J. R. 1976, *A.p.J. Suppl.*, **32**, 409.  
 Wagner, R. M., and Perrenod, S. C. 1980, preprint.

F. BARTKO: Martin Marietta Corporation, Denver Aerospace Division, P.O. Box 179, Denver, CO 80201

R. CIARDULLO and H. FORD: Astronomy Department, University of California, Los Angeles, CA 90024

R. J. HARMS: Center for Astrophysics and Space Sciences C-011, University of California, San Diego, La Jolla, CA 92093